Indonesian Journal of Electrical Engineering and Computer Science
Vol. 35, No. 1, July 2024, pp. 32~41
ISSN: 2502-4752, DOI: 10.11591/ijeecs.v35.i1.pp32-41

Grid impact analysis on wind power plant interconnection in strengthening electricity systems

Adri Senen[1,2], Arif Kurniawan[1], Hasna Satya Dini[1,2], Dwi Anggaini[1]
[1]Department of Electrical Engineering, Institut Teknologi PLN, Jakarta, Indonesia
[2]Faculty of Electrical Engineering, Universiti Teknologi Malaysia, Johor, Malaysia

Article Info

Article history:

Received Dec 17, 2023
Revised Mar 9, 2024
Accepted Mar 25, 2024

Keywords:

Frequency
Grid code
Grid impact
Intermittency
Transient stability
Wind power plant

ABSTRACT

The Timor system is one of the large systems in the East Nusa Tenggara region. Based on the general plan for electricity supply for 2021-2030, there is a plan to interconnect a 2x11 MW wind power plant. The addition of wind power plants will pose a considerable threat to the system due to the intermittency nature of renewable energy plants. Therefore, a comprehensive grid impact study is needed to convince network managers that adding wind farms will not cause disruptions to the system either locally or in general and is expected to strengthen the electricity system. The power flow simulation results, installing a 2x11 MW wind farm on the Timor system can improve voltage quality and reduce losses on both 70 and 150 kV systems. For transient stability, the frequency value on the Timor system still meets the grid code requirements. In addition, the simulation results of the intermittency impact of the wind power plant output show that the Timor system is still in a stable condition. The stability of the rotor angle of the existing power plant when the transient stability simulation is carried out shows that it is still in a balanced condition.

Corresponding Author:

Adri Senen
Department of Electrical Engineering, Institut Teknologi PLN
Jakarta, Indonesia
Email: adrisenen@itpln.ac.id

1. INTRODUCTION

Power plants in Indonesia are currently dominated by coal steam power plants, where coal is a fossil fuel that is limited in quantity and willone day run out [1], [2]. Coal cannot be used continuously as the primary fuel commodity in power plants in Indonesia because it produces significant carbon emissions and causes air pollution [1], [3], [4]. Therefore, it is necessary to take strategic steps by changing the energy paradigm, gradually reducing the use of fossil energy, reducing subsidies on energy prices, providing national energy reserves, taking responsibility for regional energy needs and prioritizing energy development [4]-[6].

One of the strateSSes to reduce carbon emissions is using renewable energy on a large scale combined with energy efficiency efforts [4], [7], [8]. Based on the general plan for electricity supply for 2021-2030, in East Nusa Tenggara province, there is a plan for a 2x11 MW wind power Timor (Scattered Quota) in the Timor system, which is planned to operate in 2024. The construction of wind farm Timor 2x11 MW aims to encourage the utilization of renewable energy generation and achieve the target of an energy mix from renewable energy of 23% renewable energy by 2025 [6]. The nature of the wind farm, whose output power depends on the wind speed, causes the output power to be intermittent [9], [10]. In addition, the wind farm can only operate if the wind speed is above the minimum limit (dead band) and below the maximum wind speed (cutoff) [11].

Understanding grid codes is essential given the rising usage of renewable energy sources, especially wind and solar energy [12]-[14]. The ability to overcome flaws is a crucial feature to take into account. Renewable power plants will be turned off instantly when system faults happen without fault ride-through capability assessments [15], [16]. If renewable energy sources are widely used, there may be significant blackouts on a large scale [17], [18]. This study helps address how the system will be impacted by increased levels of renewable energy penetration as well as for future system accuracy improvements. Intermittent generation has a high risk of uncertainty, so if its composition is above 1% of the actual load power of the system, then its presence impacts system stability. One of the stability aspects that must be considered in operating a power system with a large portion of wind power penetration is maintaining the stability of the power system, namely by maintaining the stability of the voltage profile both in transient conditions and in steady state conditions [19]-[21].

With the planned construction of a 2x11 MW wind farm in the Timor system, research is needed to apply renewable energy sources to the system because of their intermittent [22]. This nature causes generators from renewable energy sources to produce power that changes in magnitude depending on the availability of energy sources [12], [10] to know the condition of the Grid Impact of the Timor 70 kV electricity system after installing the wind farm [23]. The conditions observed in this research are the Power Flow Study on the network system before. After the wind farm is established, the observed power is in the form of active power and reactive power. The voltage profile is also observed at each bus so that there is no overvoltage or undervoltage after the wind farm is installed losses or losses are observed after the installation of the wind farm, whether the presence of losses can decrease or not, transient stability includes voltage and frequency stability [24]-[26] in the existing plant observed before and after the installation of the wind farm whether it is still in a stable condition or not. In this study, Timor system modelling, transient analysis, and load flow will be carried out with needs before and after the interconnection of a 2 x 11 MW wind farm.

2. METHOD

This research applies quantitative analysis methods. The data used in this study was obtained from the 70 kV Timor electricity system in the form of numerical data, which was then inputted and used to simulate power flow (load flow) and transient stability (frequency and rotor angle of the plant). A flowchart with thorough explanations of the study design will be presented in Figure 1.

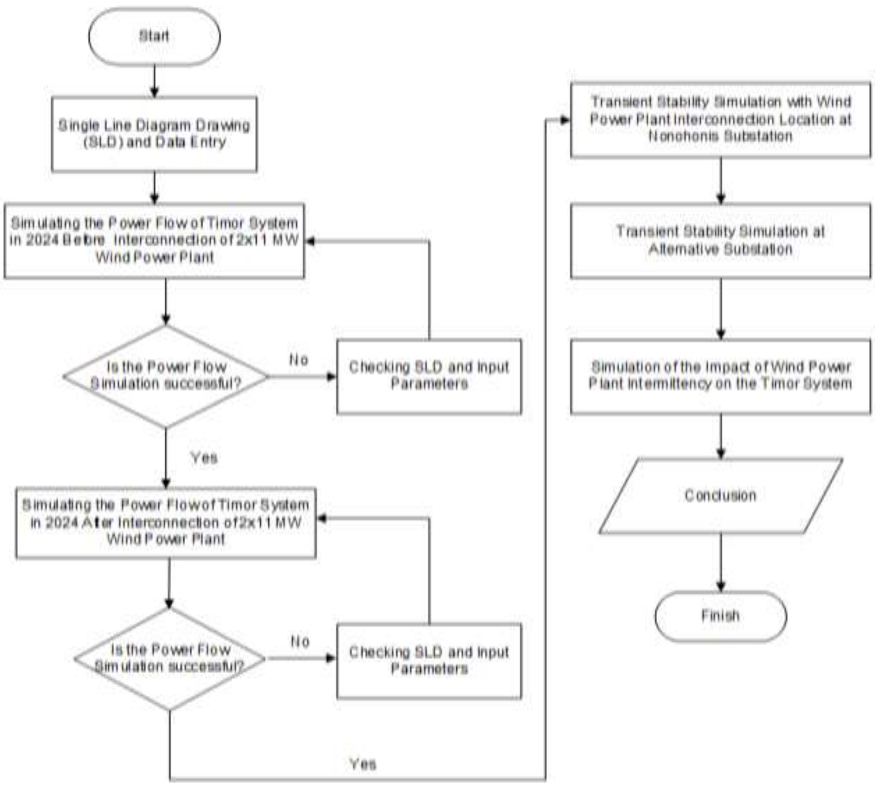

Figure 1. Research procedure

2.1. Transient stability analysis

Transient stability analysis aims to see if synchronization can be achieved after a machine has experienced a disturbance [17], [27]. Disturbances can come from sudden load shedding, plant trips, significant load losses, or other system disturbances [28]. The equal area criterion method is one way that can be used to perform stability projections quickly [29]-[31]. This approach can only be used with one-machine or two-machine systems connected on an infinite bus.

Figure 2 illustrates the general equal area criterion method where the machine operates at the equilibrium point δ_0. Figure 2 illustrates the mechanical input power $P_{m0} = P_{e0}$ for the condition. The horizontal line P_{m1} shows the rapid increase of input power. When Pm1 > P_{e0}, the rotor acceleration force is positive, and the power angle δ rises. In (1) can be used to calculate the surplus energy stored in the rotor during the first acceleration [29], [32].

$$\int_{\delta_0}^{\delta}(P_m - P_e)\ d\delta\ = area\ abc = area\ A_1 \tag{1}$$

The electrical power increases with the addition of δ, and when δ = δ1, the new input power is P_{m1}. The rotor rotates faster than the synchronous speed, even though the acceleration force is zero [18]. As a result, the power angle δ and the electrical power Pe continue to rise. Now that $P_m < P_e$, which causes the motor to decelerate towards synchronous speed until $\delta = \delta_{max}$, in (2) can be used to calculate the excess energy stored in the rotor during deceleration [11], [33].

$$\int_{\delta_1}^{max}(P_{m1} - P_e)\ d\delta\ = area\ bde = area\ A_2 \tag{2}$$

In (3) is known as the equal area criterion [34], which is derived from (1) and (2). The equal area criterion method can provide a holistic view of power system transient stability by considering all the components involved. This helps identify areas vulnerable to disturbances and enables the development of effective strategies to improve system stability.

$$|area\ A_1| = \ |area\ A_2| \tag{3}$$

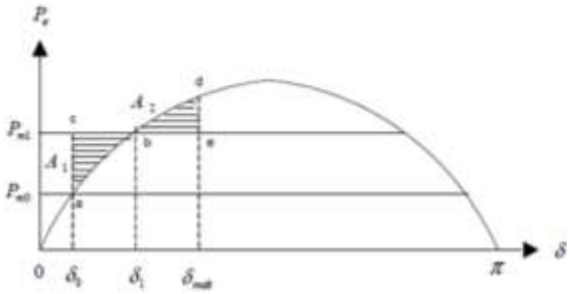

Figure 2. Equal area criteria for sudden load changes

2.2. Swing equation

The equation governs the rotation/movement of the rotor in a synchronous machine [35], [36]. It is based on the basic principles of dynamics [25], where the acceleration torque is the product of the rotor's moment of inertia (J) with its angular acceleration $(d^2\ \theta_m)/(d_t\ ^2)$ [37], [38]. The following is the rotor dynamic differential equation [2]:

$$J\frac{d^2\theta_m}{dt^2} = T_a = T_m - T_e Nm \tag{4}$$

where:
- J = Moment of inertia / total inertia of the rotor mass ($kg.m^2$)
- θm = Rotor angular displacement with respect to the stationary axis (rad)
- Ta = Net acceleration rotating moment (Nm)
- Tm = Mechanical or shaft (drive) rotating moment provided by the prime mover minus the decelerating rotating Moment caused by rotation losses (Nm)
- Te = Electrical/electromagnetic rotating Moment (Nm)

When a synchronous generator generates the electromagnetic torque under rotating conditions with synchronous speed (ωsm), $Tm = Te$, at the time of disturbance, accelerating $Tm > Te$ or decelerating $Tm < Te$ will be obtained [39], [35]. Referring to (4), where θm is determined concerning a stationary axis, the calculation of the angular position of the rotor concerning the axis of rotation with synchronous speed can be written as the following (4).

$$\theta_m = \omega_{sm} t + \delta_m \quad (5)$$

Where:
- θm = Rotor angular displacement with respect to the stationary axis (rad)
- ω_{sm} = Synchronous speed (rad/s)
- δm = Rotor angular displacement commonly called rotor angular displacement against the rotating angle/power angle of the rotating shaft at synchronous speed (radian)

In (6) is a power equation because power equals the product of rotational speed and torque (turning moment) [40].

$$J\omega_m \frac{d^2\delta_m}{dt^2} = P_m - P_e MW \quad (6)$$

Where:
- Pm is mechanical power input (MW)
- Pe is the electrical power output (MW)
- Stator copper losses are ignored.

$$\frac{H}{\pi f} \cdot \frac{d^2\delta}{dt^2} = P_m - P_e \text{ pu} \quad (7)$$

In (7) is referred to as the swing equation, which in stability studies is the basic equation governing the dynamics (motion) of synchronous machine rotation [41]. These swing equations are used to analyze the dynamic response of synchronous generators to system disturbances. This analysis helps evaluate the system's transient stability and set up protection and control systems to ensure that the generators remain in synchronization and that the power system recovers quickly after a disturbance.

3. RESULTS AND DISCUSSION

3.1. Single line diagram of Timor system

As shown in Figure 3 of the single-line diagram below, the Timor system has three voltage systems represented with different colours. A red line represents the 150 kV voltage system. The yellow line represents the 70 kV voltage system, and the brown line is the 20 kV voltage system. The addition of 2 wind farm units with a capacity of 11 MW per unit connected at the location shown in Figure 3. The selection of the wind power plant interconnection area at substation is due to geographical considerations in the middle of the Timor system and good wind potential (global wind atlas).

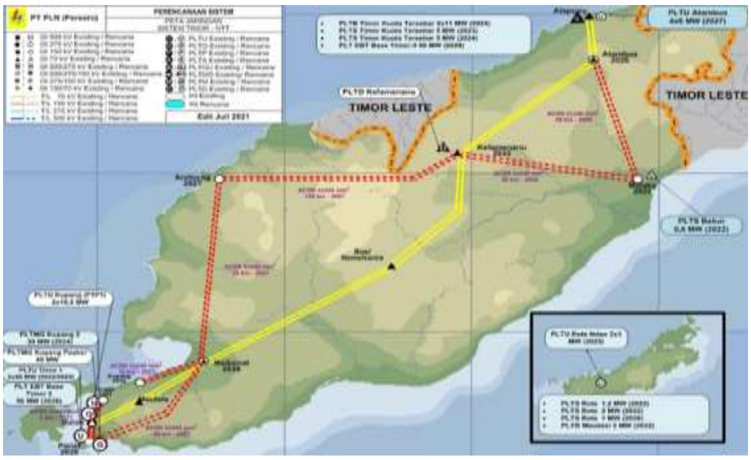

Figure 3. Single line diagram of Timor system

3.2. Simulation of load flow in the condition before and after interconnection of 2x11 MW wind power plant

The total load of the Timor system has a load value of 160.29 MW on the generation side, while on the feeder side (load P). After the power flow simulation, the total load of the Timor system has a load value of 160.29 MW on the generation side, while on the feeder side (load P), the load value is 157.7 MW. These results show the difference in the value of the load at the point of generation and load P, which is a power loss with a value of 2.59 MW.

Based on the power flow simulation results with the existing system conditions, a comparison of the conditions before and after the wind farm interconnection for parameters such as voltage and losses is obtained, as shown in Tables 1 and 2. These results show the difference in the value of the load at the point of generation and load P, which is a power loss with a value of 2.60 MW. Based on the power flow simulation results with the existing system conditions, a comparison of the conditions before and after the wind farm interconnection for parameters such as voltage and losses are obtained, as shown in Tables 1 and 2.

Table 1. Comparison of power losses in the condition before and after wind farm interconnection

No	Voltage system (kV)	Losses (MW)		
		Before	After	
			Interconnection at GI Nonohonis	Interconnection at GI Kefamenanu
1	70	5,93	2,42	1,57
2	150	0,30	0,18	0,17

Table 2. Substation (GI) voltage comparison of conditions before and after wind farm interconnection

No	Location	Voltage system (kV)	Losses (MW)		
			Before	After	
				Interconnection at GI Nonohonis	Interconnection at GI Kefamenanu
1	Bolok GI	70	66,02	69,48	70,13
2	Maulafa GI	70	65,15	69,05	69,77
3	Naibonat GI	70	64,26	69,37	70,24
4	Nonohonis GI	70	58,69	69,32	70,93
5	Kefamenanu GI	70	55,58	67,65	72,63
6	Atambua GI	70	53,13	65,75	70,90
7	Atapupu GI	70	53,04	65,68	70,84
8	Bolok GI	150	143,33	149,33	150,40
9	Panaf GI	150	143,62	149,53	150,58
10	Tenau GI	150	143,19	149,20	150,28
11	Naibonat GI	150	141,89	148,87	150,08
12	New Kupang GI	150	141,74	148,73	149,94
13	Kefamenanu GI	150	124,37	151,63	162,87
14	Malaka GI	150	124,38	151,72	162,98

The simulation results of Table 2 show that the voltage values in the Timor system at 70 kV and 150 kV voltage systems are still within the range of ± 10% voltage variation. The lowest voltage value in the 70 kV voltage system is at Atapupu GI of 65.68 kV, while the lowest voltage value in the 150 kV voltage system is at New Kupang GI of 148.73 kV. The highest voltage value in the 150 kV voltage system is at Malaka GI of 162.98 kV.

According to Tables 1 and 2, the interconnection of a 2x11 MW wind farm in the Timor system can improve voltage quality and reduce power losses for both interconnection locations at Nonohonis GI and Kefamenanu GI. The total power losses in the Timor system after the 2x11 MW wind farm interconnection is 2.60 MW, where the power losses in the 70 kV voltage system are 2.42 MW and in the 150 kV voltage system are 0.18 MW. Compared to power losses before the interconnection of 2x11 MW wind farm, power losses have decreased from 6.23 MW to 2.6 MW.

3.3. Transient stability simulation with wind power plant interconnection

Transient stability analysis to determine the voltage frequency response at the Nonohonis substation (GI) and Kefamenanu GI before and after adding wind farms. Transient simulation is carried out within 50 and will display the results through voltage, frequency and active power graphs. The simulation of the loss of 2 wind farm units has the same regulatory treatment as the simulation of the loss of 1 wind farm unit. Based on Figure 4, the scenario of losing 2x11 MW wind farm causes the frequency to drop to 49.698 Hz and the highest frequency after the system responds to the loss of 2x11 MW wind farm is 50.021 Hz. In the rotor angle graph, it can be seen that the Bolok power plant rotor angle response changes from -13.828 degrees to

9.670 degrees because the Bolok power plant compensates for the power loss of 2x11 MW. It can be seen in the graph that the Bolok power plant has the most significant change in rotor angle response.

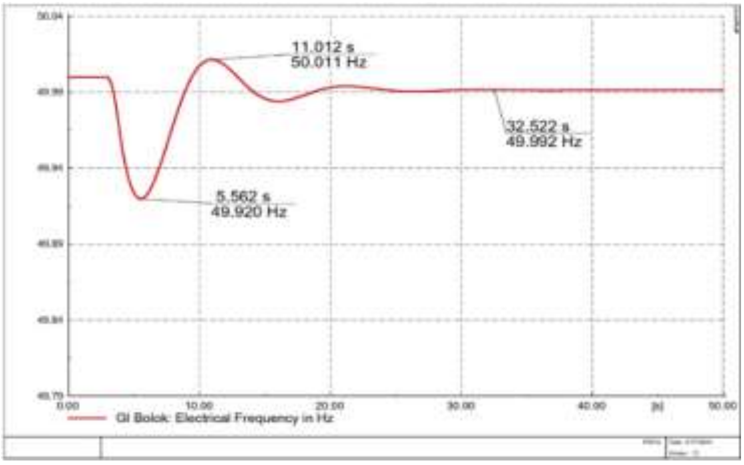

Figure 4. Timor system frequency when losing 1 unit of 11 MW wind farm with wind farm interconnection

3.4. Simulation of the impact of wind power plant intermittency on the Timor system

In this simulation, the output intermittency of a 2x11 MW wind farm will be simulated with a scenario based on the realization of a decrease in the output of Tolo wind farm with a capacity of 72 MW. This analysis is done to see how the system behaves during periods of intermittency and identify weak points (system strengths). The simulation results are shown in Figure 5.

The graph in Figure 5 is the power output profile of the Tolo wind power plant, with a capacity of 72 MW on August 28, 2021, which has the most significant decrease in power output throughout 2021. The reduction in wind farm power output occurred from 54.6 MW to 8.5 MW or 46.1 MW (64% of total capacity) in 30 minutes. In accordance with this data, the average decrease in wind farm power output per second is 25.61 kW.

Suppose the percentage decrease in power output is proportional to the capacity of the Timor wind power plant of 2x11 MW (22 MW). In that case, the decline in power output is 14.08 MW in 30 minutes, so the average decrease in power output per second is 7.82 kW. In this simulation, the power output of the Timor wind power plant will be decreased for 9 seconds so that the value of the decrease in power output is 70.38 kW (0.07038 MW). In addition, in this simulation, the setting of the wind farm power output decrease starts from the 3rd second.

The intermittency simulation is carried out by reducing the wind farm's power output from 22 MW to 21.9 MW in 9 seconds. From Figure 6, it can be seen that the decrease in power output to 21.9 MW occurred during seconds 3-12. When the wind farm output drops from 22 MW to 17.5, the lowest frequency value in the system is 49.999 Hz, and the highest frequency is 50.00014 Hz. The frequency value of the simulation results is still within the frequency range set in the Grid Code As shown in Figure 7. When there is a decrease in wind farm power output from 22 MW to 21.9 MW, the existing plants in the Timor system can still return to synchronous and stable conditions, and this can be seen from the rotor angle response of all plants in Figure 8.

Figure 5. Power output profile of 72 MW tolo wind farm

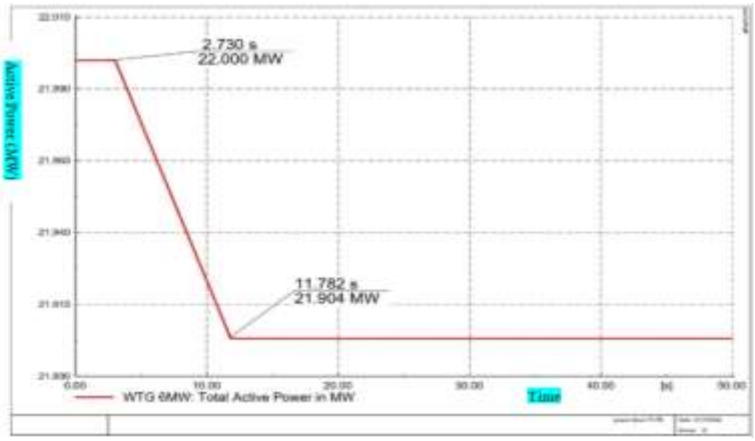

Figure 6. Decrease in wind farm output from 22 MW to 17.5 MW

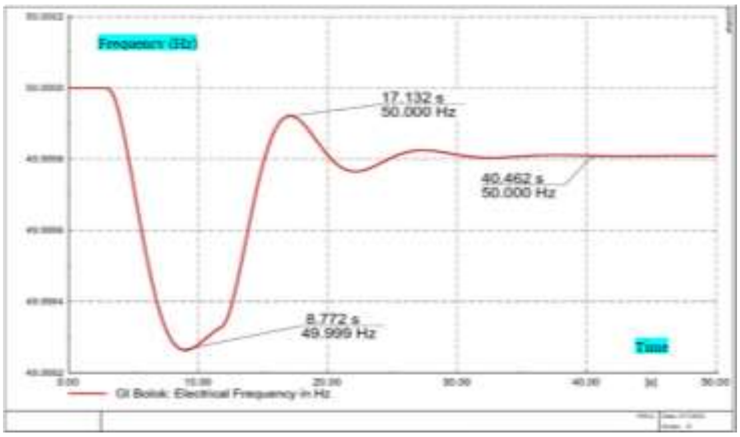

Figure 7. Timor system frequency when a wind farm output decrease from 22 MW to 22.9 MW within 9 seconds

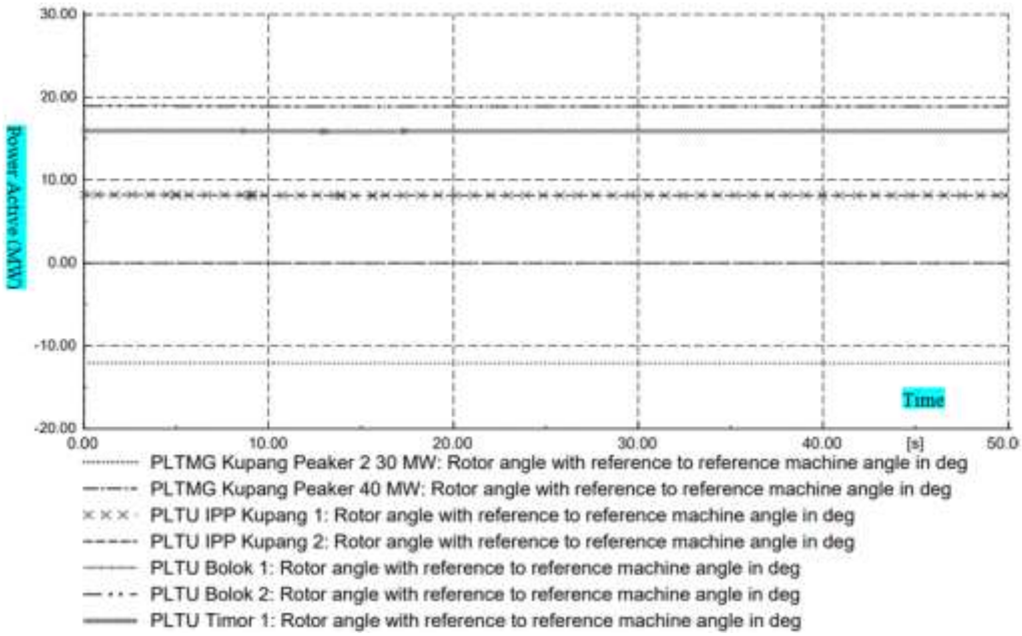

Figure 8. Generator rotor angle when a wind farm output decrease from 22 to 22.9 MW within 9 seconds

4. CONCLUSION

The installation of a 2x11 MW wind farm can improve the voltage quality of almost all substation busbars in the Timor system. When the 2x11 MW wind farm is connected to Nonohonis GI, the percentage of voltage improvement on 70 kV and 150 kV busbars is in the range of 4.17% - 24.11%. Meanwhile, when the 2x11 MW wind farm is connected to Kefamenanu GI, the percentage of voltage improvement is in the range of 4.92%-33.99%. Due to the better voltage quality, the installation of the wind farm also had an impact on reducing losses in the Timor system, where the total value of losses before the interconnection of 2x11 MW wind farm in 2024 was 6.23 MW, with losses in the 70 kV system amounting to 5.93 MW and in the 150 kV system amounting to 0.30 MW.

Based on the simulation results of the transient stability of the 2x11 MW wind farm installation, the system frequency value is still within the frequency range according to the Nusa Tenggara, Maluku, and Papua Power System Network Rules (Grid Code), namely 49.0-51.0 Hz. For the impact of wind farm intermittency, when operating normally, there may be a decrease in the most extreme output of 64% for 30 minutes from the total capacity of the wind farm. Under transient conditions, there is a change in wind farm output from 22 MW to 21.9 MW within 9 seconds. The frequency value under these conditions shows 49.99 Hz, so it is still in accordance with the Nusa Tenggara, Maluku, and Papua Power System Network Rules (Grid Code).

REFERENCES

[1] N. Reyseliani and W. W. Purwanto, "Pathway towards 100% renewable energy in Indonesia power system by 2050," *Renewable Energy*, vol. 176, pp. 305–321, Oct. 2021, doi: 10.1016/j.renene.2021.05.118.

[2] R. Clark, N. Zucker, and J. Urpelainen, "The future of coal-fired power generation in Southeast Asia," *Renewable and Sustainable Energy Reviews*, vol. 121, p. 109650, Apr. 2020, doi: 10.1016/j.rser.2019.109650.

[3] P. Oskarsson, K. B. Nielsen, K. Lahiri-Dutt, and B. Roy, "India's new coal geography: Coastal transformations, imported fuel and state-business collaboration in the transition to more fossil fuel energy," *Energy Research & Social Science*, vol. 73, p. 101903, Mar. 2021, doi: 10.1016/j.erss.2020.101903.

[4] L. Sani, D. Khatiwada, F. Harahap, and S. Silveira, "Decarbonization pathways for the power sector in Sumatra, Indonesia," *Renewable and Sustainable Energy Reviews*, vol. 150, p. 111507, Oct. 2021, doi: 10.1016/j.rser.2021.111507.

[5] K. Grimsrud, C. Hagem, A. Lind, and H. Lindhjem, "Efficient spatial distribution of wind power plants given environmental externalities due to turbines and grids," *Energy Economics*, vol. 102, p. 105487, Oct. 2021, doi: 10.1016/j.eneco.2021.105487.

[6] H. B. Tambunan *et al.*, "The challenges and opportunities of renewable energy source (RES) penetration in Indonesia: case study of Java-Bali power system," *Energies*, vol. 13, no. 22, p. 5903, Nov. 2020, doi: 10.3390/en13225903.

[7] K. Yu and P. van Son, "Review of trans-mediterranean power grid interconnection: a regional roadmap towards energy sector decarbonization," *Global Energy Interconnection*, vol. 6, no. 1, pp. 115–126, Feb. 2023, doi: 10.1016/j.gloei.2023.02.010.

[8] S. Hoseinzadeh, D. Astiaso Garcia, and L. Huang, "Grid-connected renewable energy systems flexibility in Norway islands' decarbonization," *Renewable and Sustainable Energy Reviews*, vol. 185, p. 113658, Oct. 2023, doi: 10.1016/j.rser.2023.113658.

[9] M. Elsisi, M.-Q. Tran, K. Mahmoud, M. Lehtonen, and M. M. F. Darwish, "Robust design of ANFIS-based blade pitch controller for wind energy conversion systems against wind speed fluctuations," *IEEE Access*, vol. 9, pp. 37894–37904, 2021, doi: 10.1109/ACCESS.2021.3063053.

[10] S. Mokeke and L. Z. Thamae, "The impact of intermittent renewable energy generators on Lesotho national electricity grid," *Electric Power Systems Research*, vol. 196, p. 107196, Jul. 2021, doi: 10.1016/j.epsr.2021.107196.

[11] H. R. Shabani and M. Kalantar, "Real-time transient stability detection in the power system with high penetration of DFIG-based wind farms using transient energy function," *International Journal of Electrical Power & Energy Systems*, vol. 133, p. 107319, Dec. 2021, doi: 10.1016/j.ijepes.2021.107319.

[12] S. D. Ahmed, F. S. M. Al-Ismail, M. Shafiullah, F. A. Al-Sulaiman, and I. M. El-Amin, "Grid integration challenges of wind energy: a review," *IEEE Access*, vol. 8, pp. 10857–10878, 2020, doi: 10.1109/ACCESS.2020.2964896.

[13] M. T. Mito, X. Ma, H. Albuflasa, and P. A. Davies, "Modular operation of renewable energy-driven reverse osmosis using neural networks for wind speed prediction and scheduling," *Desalination*, vol. 567, p. 116950, Dec. 2023, doi: 10.1016/j.desal.2023.116950.

[14] J. L. de Souza Silva *et al.*, "Case study of photovoltaic power plants in a model of sustainable university in Brazil," *Renewable Energy*, vol. 196, pp. 247–260, Aug. 2022, doi: 10.1016/j.renene.2022.06.103.

[15] C. O'Malley, P. de Mars, L. Badesa, and G. Strbac, "Reinforcement learning and mixed-integer programming for power plant scheduling in low carbon systems: comparison and hybridisation," *Applied Energy*, vol. 349, p. 121659, Nov. 2023, doi: 10.1016/j.apenergy.2023.121659.

[16] M. Abdullah-Al-Mahbub and A. R. M. T. Islam, "Current status of running renewable energy in Bangladesh and future prospect: a global comparison," *Heliyon*, vol. 9, no. 3, p. e14308, Mar. 2023, doi: 10.1016/j.heliyon.2023.e14308.

[17] T. G. Magallones and J. Govind Singh, "Impact of interconnections and renewable energy integration on the Philippine–Sabah power grid systems," *Global Energy Interconnection*, vol. 6, no. 3, pp. 253–272, Jun. 2023, doi: 10.1016/j.gloei.2023.06.001.

[18] D. W. Gao, Z. Wu, W. Yan, H. Zhang, S. Yan, and X. Wang, "Comprehensive frequency regulation scheme for permanent magnet synchronous generator-based wind turbine generation system," *IET Renewable Power Generation*, vol. 13, no. 2, pp. 234–244, Feb. 2019, doi: 10.1049/iet-rpg.2018.5247.

[19] S. Niu, Z. Zhang, X. Ke, G. Zhang, C. Huo, and B. Qin, "Impact of renewable energy penetration rate on power system transient voltage stability," *Energy Reports*, vol. 8, pp. 487–492, Apr. 2022, doi: 10.1016/j.egyr.2021.11.160.

[20] H. Tian, H. Liu, H. Ma, P. Zhang, X. Qin, and C. Ma, "Steady-state voltage-control method considering large-scale wind-power transmission using half-wavelength transmission lines," *Global Energy Interconnection*, vol. 4, no. 3, pp. 239–250, Jun. 2021, doi: 10.1016/j.gloei.2021.07.009.

[21] R. Sakipour and H. Abdi, "Voltage stability improvement of wind farms by self-correcting static volt-ampere reactive compensator and energy storage," *International Journal of Electrical Power & Energy Systems*, vol. 140, p. 108082, Sep. 2022, doi: 10.1016/j.ijepes.2022.108082.

[22] X. Ge, J. Qian, Y. Fu, W.-J. Lee, and Y. Mi, "Transient stability evaluation criterion of multi-wind farms integrated power system," *IEEE Transactions on Power Systems*, vol. 37, no. 4, pp. 3137–3140, Jul. 2022, doi: 10.1109/TPWRS.2022.3156430.

[23] S. Saha, M. I. Saleem, and T. K. Roy, "Impact of high penetration of renewable energy sources on grid frequency behaviour," *International Journal of Electrical Power and Energy Systems*, vol. 145, 2023, doi: 10.1016/j.ijepes.2022.108701.

[24] J. Huang *et al.*, "Interconnection-level primary frequency control by MBPSS with wind generation and evaluation of economic impacts," *International Journal of Electrical Power & Energy Systems*, vol. 119, p. 105867, Jul. 2020, doi: 10.1016/j.ijepes.2020.105867.

[25] A. Schwanka Trevisan, A. Mendonça, R. Gagnon, M. Fecteau, and J. Mahseredjian, "Assessment of interactions involving wind farms in large-scale grids," *Electric Power Systems Research*, vol. 196, p. 107220, Jul. 2021, doi: 10.1016/j.epsr.2021.107220.

[26] X. Zhao, Y. Xue, and X.-P. Zhang, "Fast frequency support from wind turbine systems by arresting frequency nadir close to settling frequency," *IEEE Open Access Journal of Power and Energy*, vol. 7, pp. 191–202, 2020, doi: 10.1109/OAJPE.2020.2996949.

[27] N. Hatziargyriou *et al.*, "Definition and classification of power system stability – revisited & extended," *IEEE Transactions on Power Systems*, vol. 36, no. 4, pp. 3271–3281, Jul. 2021, doi: 10.1109/TPWRS.2020.3041774.

[28] A. Salah Saidi, "Impact of grid-tied photovoltaic systems on voltage stability of tunisian distribution networks using dynamic reactive power control," *Ain Shams Engineering Journal*, vol. 13, no. 2, p. 101537, Mar. 2022, doi: 10.1016/j.asej.2021.06.023.

[29] Z. Gao, W. Du, and H. F. Wang, "Transient stability analysis of a grid-connected type-4 wind turbine with grid-forming control during the fault," *International Journal of Electrical Power & Energy Systems*, vol. 155, p. 109514, Jan. 2024, doi: 10.1016/j.ijepes.2023.109514.

[30] H. M. Hasanien, M. Tostado-Véliz, R. A. Turky, and F. Jurado, "Hybrid adaptive controlled flywheel energy storage units for transient stability improvement of wind farms," *Journal of Energy Storage*, vol. 54, p. 105262, Oct. 2022, doi: 10.1016/j.est.2022.105262.

[31] B. B. Adetokun, C. M. Muriithi, and J. O. Ojo, "Voltage stability assessment and enhancement of power grid with increasing wind energy penetration," *International Journal of Electrical Power & Energy Systems*, vol. 120, p. 105988, Sep. 2020, doi: 10.1016/j.ijepes.2020.105988.

[32] A. Sinha and A. K. Samantaray, "Escape through parametric instabilities in a non-ideal motor driven geared rotor shaft driveline," *Mechanism and Machine Theory*, vol. 180, p. 105166, Feb. 2023, doi: 10.1016/j.mechmachtheory.2022.105166.

[33] A. Iqbal, V. Chitturi, and K. V. L. Narayana, "A novel vertical axis wind turbine for energy harvesting on the highways," in *2019 Innovations in Power and Advanced Computing Technologies (i-PACT)*, IEEE, Mar. 2019, pp. 1–5. doi: 10.1109/i-PACT44901.2019.8959953.

[34] S. Batchu, Y. Raghuvamsi, and K. Teeparthi, "A comparative study on equal area criterion based methods for transient stability assessment in power systems," in *2022 22nd National Power Systems Conference (NPSC)*, IEEE, Dec. 2022, pp. 124–129. doi: 10.1109/NPSC57038.2022.10069303.

[35] H. Z. Agrebi *et al.*, "Integrated optimal design of permanent magnet synchronous generator for smart wind turbine using genetic algorithm," *Energies*, vol. 14, no. 15, p. 4642, Jul. 2021, doi: 10.3390/en14154642.

[36] M. N. Pala, A. Thakar, and A. Patel, "Power swing and out of step protection using equal area criteria," in *2019 IEEE 5th International Conference for Convergence in Technology (I2CT)*, IEEE, Mar. 2019, pp. 1–7. doi: 10.1109/I2CT45611.2019.9033717.

[37] J. Li, C. Liu, P. Zhang, Y. Wang, and J. Rong, "Difference between grid connections of large-scale wind power and conventional synchronous generation," *Global Energy Interconnection*, vol. 3, no. 5, pp. 486–493, Oct. 2020, doi: 10.1016/j.gloei.2020.11.008.

[38] W. Bao, L. Ding, Y. C. Kang, and L. Sun, "Closed-loop synthetic inertia control for wind turbine generators in association with slightly over-speeded deloading operation," *IEEE Transactions on Power Systems*, vol. 38, no. 6, pp. 5022–5032, Nov. 2023, doi: 10.1109/TPWRS.2022.3224431.

[39] Y.-K. Wu, K. Le, T.-A. Nguyen, and O.-D. Phan, "Estimation of power system inertia using traditional swing equation, polynomial approximation and RV methods," in *2020 International Symposium on Computer, Consumer and Control (IS3C)*, IEEE, Nov. 2020, pp. 347–350. doi: 10.1109/IS3C50286.2020.00096.

[40] H. Cheng, Z. Shuai, C. Shen, X. Liu, Z. Li, and Z. J. Shen, "Transient angle stability of paralleled synchronous and virtual synchronous generators in islanded microgrids," *IEEE Transactions on Power Electronics*, vol. 35, no. 8, pp. 8751–8765, Aug. 2020, doi: 10.1109/TPEL.2020.2965152.

[41] B. Mohanty, S. Dhople, and K. A. Stelson, "A dynamical model for a hydrostatic wind turbine transmission coupled to the grid with a synchronous generator," in *2019 American Control Conference (ACC)*, IEEE, Jul. 2019, pp. 5774–5779. doi: 10.23919/ACC.2019.8814746.

BIOGRAPHIES OF AUTHORS

Adri Senen received the bachelor's degree in electrical engineering from Andalas University, Indonesia in 2004, and Master Degree in electrical power engineering from Bandung Insitute of Technology (ITB), Indonesia in 2008. Currently he is a Ph.D. student in School of Electrical Engineering in Universiti Teknology Malaysia, and he is a lecturer at the Institut Teknology PLN since 2017. His research interests concern load forecasting, management energy, electrical planning, renewable energy, and power system. He can be contacted at email: adrisenen@itpln.ac.id.

Arif Kurniawan was born in Jakarta on April 27, 1986. Received a Diploma from Polytechnic Negeri Jakarta in 2007, and a bachelor's degree from PLN Institute of Technology in 2022. Started working at PT PLN (Persero) in 2009 as a junior engineer of distribution network planning, as a junior electrical generator in 2010, as a junior engineer of SCADA and Telecommunication in 2011 as a junior engineer of planning, and junior engineer of electrical investment planning. Currently working in the finance department focusing on planning the funding of electricity infrastructure projects at PT. PLN (Persero). He can be contacted at email: arif.kurniawan@pln.co.id.

Hasna Satya Dini received the Bachelor and master's degree in electrical enginering from Institut Teknology Bandung, Indonesia in 2016 and 2017. She is currently pursuing a PhD student in School of Electrical Engineering in Universiti Teknology Malaysia. Her research interests mainly focus on resiliency, optimization, and power system stability. She can be contacted at email: hasna@itpln.ac.id.

Dwi Anggaini received the Bachelor Degree in Mathematics Education (S. Pd) from Muhammadiyah University Prof. Dr. HAMKA, Indonesia in 2012, and Master Degree in Reseach and Evaluation of Education (M.Pd) from Graduate school of Muhammadiyah University Prof. Dr. HAMKA, Indonesia in 2015. Currently she is a lecturer at the Institut Teknology PLN since 2017 and has developed several studies including education, statistics, data analysis and applied mathematics. She can be contacted at email: dwi_anggaini@itpln.ac.id.